Available online at www.sciencedirect.com
ScienceDirect
Journal of the European Ceramic Society 29 (2009) 3147–3158
www.elsevier.com/locate/jeurceramsoc

Post-deposition laser treatment of plasma sprayed titania-hydroxyapatite functionally graded coatings

V. Cannillo [a], L. Lusvarghi [a], A. Sola [a,*], M. Barletta [b]

[a] *Dipartimento di Ingegneria dei Materiali e dell'Ambiente, Università di Modena e Reggio Emilia, Via Vignolese 905, 41100 Modena (MO), Italy*
[b] *Dipartimento di Ingegneria Meccanica, Università di Roma Tor Vergata, Via del Politecnico 1, 00133 Roma, Italy*

Received 3 March 2009; received in revised form 19 May 2009; accepted 30 May 2009
Available online 4 July 2009

Abstract

The viability of a high power diode laser source as effective post-deposition treatment technique of functionally graded titania-HA coatings was checked. In particular, several laser treatments were performed on various coatings plasma-sprayed under different conditions to verify the presence of an operative window large enough for practical purposes and, subsequently, to identify the most promising settings of the laser parameters. Laser power as low as 80–100 W and focus distance as high as −4 mm were found to be the most feasible choice to improve the overall coating properties as well as to inhibit undesired secondary reactions between calcium phosphates and titania. Finally, the best set of the laser parameters were applied to a pure HA coating and to a titania-HA graded one, plasma-sprayed under the same conditions, to perform a comparative evaluation.

The microstructural characterization by scanning electron microscopy, X-ray diffraction and the local mechanical investigation by Vickers micro-indentations proved that the degree of crystallinity of HA at the outermost layers of the graded coating could be improved without significantly altering the compositional and functional gradient. Furthermore, the properties of the pure HA coating, as-sprayed and laser treated, were found to be substantially less advantageous than those of the titania-HA functionally graded coating (higher microstructural defectiveness; inferior degree of crystallinity of HA at the working surface; lower Vickers hardness), thus confirming the beneficial effect of the compositional gradient.

Keywords: Microstructure-final; Apatite; TiO_2; Functionally graded coatings; Laser treatment

1. Introduction

Hydroxyapatite (HA) is commonly applied in biomedical devices, since its chemical composition ($Ca_5(PO_4)_3(OH)$) and mineralogical nature are quite similar to those of the mineral component of human bones, favouring the integration of artificial prostheses into the hosting natural tissue. In spite of its good bioactivity, HA suffers from its relatively poor mechanical properties, especially its brittleness, which limit its usage to not load-bearing applications. To overcome this drawback, HA is mainly used as a coating onto metal substrates, typically titanium and titanium alloys, which provide the implant with the required mechanical solidity.[1]

At present, thermal spray techniques and, in particular, plasma spraying are the most popular techniques to deposit HA coatings onto metal substrates.[2,3] The success of plasma spraying in the industrial practice greatly relies on its flexibility, reliability and time/cost/result balance.[4] However, it is known from the literature that the interface between the HA coating and the metal substrate may be defective, sensibly reducing the durability of the implant.[1] Moreover, the very high temperatures involved in the plasma flux are likely to cause a (partial) thermal decomposition of HA, promoting an uncontrolled development of by-products such as tri- and tetra-calcium phosphates and even CaO; the presence of an amorphous phosphate phase is probable as well.[1] Since the coating adhesion and its microstructural properties (such as final composition and degree of crystallinity) deeply influence the performance of biomedical devices, the deposition parameters must be strictly controlled in order to optimise the coating.[1]

A further improvement may be achieved by introducing a proper bond coat.[2,5,6] For example, Heimann et al. proved that the interposition of a titania layer increases the coating adhesion, thanks to the affinity of titania to the titanium substrate,

* Corresponding author. Tel.: +39 059 2056229; fax: +39 059 2056243.
E-mail address: antonella.sola@unimore.it (A. Sola).

0955-2219/$ – see front matter © 2009 Elsevier Ltd. All rights reserved.
doi:10.1016/j.jeurceramsoc.2009.05.053

and improves the crystallinity of the HA top layer, by reducing its cooling rate during deposition (the thermal conductivity of titania is lower than that of titanium) and avoiding the direct contact with titanium which is thought to catalyse the decomposition of HA.[5]

The crystallinity of HA can be enhanced also via an appropriate post-deposition thermal treatment.[7] Recently, laser treatments have been increasingly investigated as an alternative solution, since they are extremely quick and highly localized.[8–12] Their main advantage with respect to traditional thermal treatments is their effectiveness on a limited portion of the substrate-coating system, which makes it possible to treat just the coating or a selected zone of it, without involving (and altering) the substrate.[13] Practical advantages of the laser treatments include generally small treating system, limited manipulations and transportations of the components to be treated, environmental and operative safety, low running cost and energy consumption.[14]

Yet, laser treatments of thermally sprayed coatings are affected by several drawbacks still without solution, which are mostly ascribable to their aptitude for operating at too high fluence (power per unit of time and surface).[15] The thermal shock induced by the high-density power laser radiation into the thermal-sprayed coatings may induce massive damages, with horizontal and vertical cracks spreading widely.[9] Indeed, brittle failure of the whole coating is not a rare event.[16] The densification and recrystallization of the outermost layers of the laser treated thermally sprayed coatings may correspond to an increase in porosity and defectiveness in their innermost layers.[17] Finally, severe burns of the surfaces exposed to the radiation with the concurrent change in their aesthetic appeal are not unusual.[17]

The diode laser is based on a relatively novel source, which is characterized by a rather large spot size ($\sim$3.5 mm^2) and a peculiar power distribution.[18] It has the capability to work in defocused conditions, as well. Hence, its power surplus can be accurately controlled, thus limiting the potentially detrimental effects of the thermal shock and/or of the excess of heat delivered onto the surface to be treated. This makes the diode laser an extremely promising system for the selective heat treatment of thermally sprayed coatings.

This is, therefore, the context in which the present research aims at probing the effect of a post-deposition treatment on innovative plasma-sprayed titania-HA functionally graded coatings[19,20] by using a high power diode laser system. In particular, several laser treatments were performed on coatings plasma-sprayed under different conditions to verify the presence of an operative window large enough for practical purpose and, subsequently, to identify the most promising settings of the laser parameters. The performance of the laser treatments was estimated in terms of the changes they were able to bring into the microstructure and composition of the different thermally sprayed coatings. Further, the evolution of the mechanical properties of the coatings according to the laser operational choices was always looked into. Such study allowed the determination of the best set of laser parameters, which were subsequently applied to a pure HA coating and to a titania-HA graded coating, plasma-sprayed under the same conditions, to perform a comparative evaluation.

In the context of the assessment of the titania-HA graded coatings, the present research brings an original contribution by investigating the results of the interaction between them and the new-generation laser treatments.

2. Materials and methods

2.1. Plasma-spraying of titania-HA graded coatings

Titania-HA graded coatings ($\sim$200 μm thick) were plasma-sprayed onto 5 mm × 23 mm × 23 mm Ti6Al4V substrates using a F4-MB plasma torch. In order to create the graded coatings (nearly continuous variation in the coating composition from the substrate to the coating surface), the titania and HA powders were separately injected through the gun by two separate feeders and the feeding rates were gradually changed by progressively increasing the amount of HA and reducing the amount of titania supplied. Such efforts led to coatings all showing the same compositional gradient, that is, from pure titania at the interface with the Ti6Al4V substrate to pure HA at the working surface. Fig. 1 depicts the characteristic of the functionally graded HA-titania coatings.

As reported in a previous study,[20] although the compositional gradient of the plasma-sprayed HA-titania coatings remained similar, different spraying conditions (i.e. plasma torch power, hydrogen flux and spraying distance) could lead to different coating properties in terms of microstructure (porosity, cracks and defects, adhesion at the interface with the substrate, ...) and degree of crystallinity of the pure HA at the working surface.[20] Table 1 summarizes the most relevant spraying parameters which were set in the manufacturing of the coatings used in the present investigation and the corresponding properties. As described in previous studies,[20] the microstructure indicator of the graded coatings was expressed by a pool of experts in ceramic coatings, which gave marks ranging from 1 (bad microstructure) to 4 (very good microstructure). The microstructural evaluation was based on both the appearance of the coatings

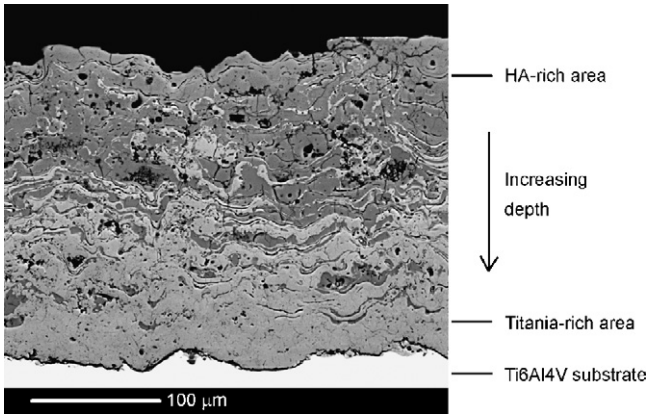

Fig. 1. SEM image of the FGM C cross section, exemplifying the compositional gradient. In spite of the differences proposed in Table 1, the compositional gradient of all the FGMs considered here can described by this "scheme".

Table 1
Spraying parameters applied to produce the coatings and corresponding properties.

Sample	Spraying parameters			Coatings properties	
	Torch power (kW)	H_2 flux (S.L.P.M.)	Distance (mm)	Microstructure indicator[a]	HA crystallinity (%)
FGM A	38	15	90	2.50/4	40.1 ± 0.9
FGM B	42	5	110	1.67/4	47.3 ± 0.1
FGM C	40	15	100	3.33/4	36.0 ± 1.0
FGM*	38	5	90	3.33/4	50.6 ± 0.1
HA*	38	5	90	N.A.	43.0 ± 1.0

[a] The microstructure indicator ranged from 1 (bad microstructure) to 4 (very good microstructure).

(a common practice in Design of Experiments procedures, which are intended to rationalise the experimental activity thanks to a statistical approach[21]) and quantitative data, such as the mean thickness and porosity content, which were measured via a SEM image analysis.[20] Table 1 also lists the relative degree of crystallinity of the HA at the working surface of the coatings. This parameter was deduced by XRD tests carried out on the surface of the graded coatings. The patterns were collected in the 20–60° 2θ range, working with a Cu Kα radiation with a scanning rate of 0.02°/s. The relative degree of crystallinity was calculated by comparing the main peak intensity I of the XRD pattern of the coating and the main peak intensity I_{HA} of the XRD pattern of the HA feedstock powder[22]:

$$\text{Relative Degree of Crystallinity}(\%) = \frac{I}{I_{HA}} \cdot 100 \quad (1)$$

Eq. (1) may be considered as a quantitative means to compare the coatings, since it provides a normalized peak intensity which is an indicator of the crystallinity preserved by the HA on the working surface.[20,22]

Therefore, to comprehensively study the interaction mechanisms between the laser source and the plasma-sprayed HA-titania coatings whatever the settings of the plasma spraying, several set of samples coated under different operational plasma-spraying parameters were chosen. They can be classified as follows:

- FGM A: good compromise between microstructural quality and degree of crystallinity of HA;
- FGM B: high crystallinity but modest microstructure;
- FGM C: good microstructure but modest crystallinity.

An additional set of samples, namely, FGM*, which, according to the past studies,[20] had the best properties in terms of microstructure and HA crystallinity, was submitted to the laser treatments under selected operational parameters and the interaction mechanisms between the laser beam and the coatings were further investigated.

Finally, comparative laser treatments were performed on a pure HA coating plasma-sprayed using the same deposition parameters as FGM*. The comparison between the pure HA coatings (HA*) and the FGM coatings (FGM*) was looked into to emphasize how the effect of the compositional gradient could influence the interaction mechanisms between the laser beam and the coatings.

2.2. Heat treating by laser

In order to perform the laser treatments, the thermal-sprayed samples (squares, about 20–25 mm wide) were simply rinsed in acetone, to remove any grease residue, and used as-sprayed (no polishing of the surface was carried out, since such operation would remove the HA-rich layers of the coating, altering the compositional gradient). In this way, all the coatings (before laser treatment) presented the lamellar microstructure typical of thermal-sprayed coatings. To the naked eye, they all appeared grey in colour and very rough.

Surface laser treatments were performed using an HPDL Rofin-Sinar model DL015 with a maximum power of 1500 W, wavelength of 940 nm, elliptic spot of 0.6 along the minor axis and 1.9 along the major axis. A 63 mm long focus lens was selected to guarantee and improve the ability of the laser beam to penetrate a greater thickness of the plasma-sprayed coating. During the processing, the samples were held on a CNC movement system and treated by moving them under the motionless laser source. The work area (X–Y plane) was 350 × 350 mm with an upright clearance of 300 mm and a Z axis stroke of 50 mm. In the present contribution, each scanning path was 20 mm long. However it is worth noting that the laser treatment can be easily scaled up to large devices, also characterized by complex geometrical shapes. For protection and insulation purposes, an inert gas (Argon) flux was also directed on the sample surface.

Surface heat treatments followed the experimental schedule reported in Table 2. The experimental factors investigated were laser power, scan speed, focus, and number of passes. The set of laser parameters leading to the best results in terms of final coatings composition, microstructure and degree of crystallinity were looked for.

2.3. Characterization tests

The morphology of titania-HA plasma-sprayed coatings before and after the laser treatments was investigated by environmental scanning electron microscopy, ESEM (Quanta FEI 2000), operated in low-vacuum mode (0.5 Torr pressure) to avoid metallization of the surface. X-ray energy dispersion spectroscopy X-EDS (Oxford Inca 350) was used to check the presence of microscopic compositional variations in the laser treated coatings. The cross sections of the coatings before and after the laser treatments were observed at different magnification by ESEM to emphasize change in their microstructure as

Table 2
Post-deposition laser treatments performed on the preliminary samples.

Parameters of the laser treatment				Treated FGM samples		
Defocus (mm)	Power (W)	Speed (mm/s)	Passes (number)	FGM A	FGM B	FGM C
No	500	3	1	/	Yes	/
No	200	3	1	Yes	/	/
No	200	5	1	Yes	/	/
No	150	7	1	/	Yes	/
No	120	3	1	Yes	/	/
No	100	3	1	Yes	Yes[a]	Yes
No	100	5	1	Yes	Yes	Yes
No	100	7	1	/	Yes	/
No	90	3	1	/	/	Yes
No	80	3	1	Yes	Yes	Yes[a]
No	80	5	1	/	/	Yes
No	80	3	2	Yes	/	/
No	80	5	2	Yes	/	/
−2	150	3	1	/	Yes	Yes
−2	130	3	1	Yes	Yes	Yes
−2	100	3	1	Yes	Yes	Yes
−2	100	3	2	Yes	Yes	Yes
−4	200	3	1	Yes	Yes	Yes
−4	150	3	1	Yes	Yes	Yes
−4	100	3	1	Yes	Yes	Yes
−4	150	3	2	Yes	Yes	Yes
−4	100	3	2	/	Yes	/
−4	100	3	4	Yes	Yes	/

Columns on the left: parameters used (defocalization distance; power; traverse speed; number of passes); columns on the right: samples subjected to the specific laser treatment.

[a] Tests repeated more than once in order to check the reproducibility of the laser treatments.

well as to examine the level of their defectiveness (cracks, porosity, . . .). X-ray diffraction XRD (PANalytical X'pert PRO) was performed using Cu Kα radiation, working in the 20–70° 2 theta range, step size 0.017° and scan step time 61.325 s. This way, the change in the composition and in the degree of crystallinity of the laser treated samples can be accurately estimated.

The mechanical properties of FGM* and HA* coatings were characterized by Vickers micro-hardness (Wolpert Group, Micro-Vickers Hardness Tester digital auto turret, Mod. 402MVD), 100 g_f (HV 0.1) maximum load. The indentations were performed along the cross section of the coatings at different distances from the working surface. This clarified the effect of the functional gradient induced by the spatial compositional change inside the coatings and, eventually, the outcome of the laser treatments.

3. Results and discussion

3.1. Preliminary tests

In order to explore the effect of the laser treatments (with various processing conditions) on the graded coatings, an intensive characterization campaign was carried out, taking into account both the presence of the compositional gradient in the samples[23] and the wide range of beam-matter interactions that may occur.[24]

A first evaluation was based on the aesthetic appearance of the samples, which can be markedly modified by the laser treatment. In several studies dedicated to thermal-sprayed coatings, for example, it has been observed that a high-density power radiation may cause significant alterations, accompanied by horizontal and vertical cracks[9]; also sever burns, immediately appreciable to the naked eyes, are common.[17] As a consequence, the development of burnt areas or the widespread propagation of cracks and defects could be considered as an indication of an excessive exposition to the laser radiation.[17] Even if the result of various treatments carried out in the present research was visible, all the "laser tracks" were observed by SEM and analysed by XRD. This was helpful to interpret the effect of those laser treatments which did not burn the coatings, but significantly changed them causing the development of white and flat surfaces. In fact, as discussed in the following, the SEM and XRD investigation related such modifications to the development of new crystalline phases, such as calcium titanate and tri-calcium phosphates. Instead, those coatings which appeared unchanged to the naked eyes generally preserved the HA on their surface and, if the laser parameters were appropriate, an increased crystallinity was observed.

Based on the experimental data acquired, some basic considerations can be drawn. First of all, the same laser treatment, performed on different FGMs, can give place to slightly different results. This is reasonable, since the compositional gradient is the same, but the graded coatings, as reported in Table 1, differ because of their microstructural peculiarities and, most of all, their degree of crystallinity of HA at the working surface.

Even if different FGMs can respond to the same treatment in different ways, it was apparent how high-power treatments were detrimental to the coating properties. For example, Fig. 2a is a photograph of FGM B treated at 500 W, in focus, 3 mm/s, 1 pass.

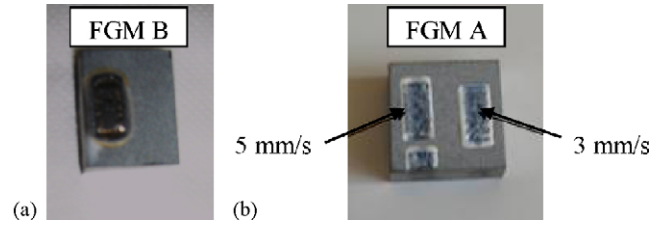

Fig. 2. Effect of high-power laser treatments: (a) FGM B treated at 500 W (in focus; 3 mm/s; 1 pass); (b) FGM A treated at 200 W (in focus; 5 mm/s on the left and 3 mm/s on the right; 1 pass). Each sample is about 2.5 cm × 2.5 cm.

The graded coating was spoilt (severe burns) by the laser treatment and the titanium alloy substrate was left unprotected. The laser treatments performed at 200 W were less destructive, but they still over-heated the samples (FGM A reported in Fig. 2b). This is a significant result, because it proves how the effect of different scanning speeds (3 and 5 mm/s) was not influential in establishing the coating characteristics at high power. In fact, the two "laser tracks" produced at 200 W, at 3 and 5 mm/s, were both detrimental and undistinguishable to the naked eye. The close similarity was confirmed by the XRD and ESEM characterization (not shown).

In order to avoid such a severe alteration of the graded coatings, lower values of the laser power were required. As a consequence, laser treatments were performed at 100 W and also 80 W. Moreover various scanning speeds were tested.

The results of the treatments at 100 W are presented in Fig. 3. By decreasing the laser power to 100 W, white surfaces were obtained and the substrate was not left unprotected any more. However, the "laser tracks" were slightly different on the different samples investigated: their appearance was particularly white, compact and homogeneous on FGM B, but it was less uniform on FGM A and even less on FGM C. This difference was presumably ascribable to the different initial degree of crystallinity of the samples, since FGM B was the most crystalline one, while FGM C was the least, as reported in Table 1. Fig. 3 also emphasizes the effect of the scanning speed; by increasing the speed, less flat and more irregular "tracks" were produced. This is probably due to the fact that higher scanning speeds resulted in shorter interaction times, impeding a uniform treatment of the coating.

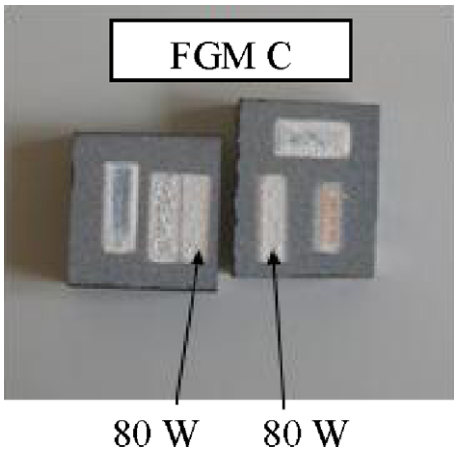

Fig. 4. Low-power laser treatment, at 80 W, on FGM C (in focus position; 3 mm/s scan speed; 1 pass). The test was performed twice to check the repeatability.

A further reduction in the laser power to 80 W resulted in a softer treatment, as shown in Fig. 4: the "laser track" on FGM C exhibited a grey central area at 100 W, but not at 80 W. Moreover the areas treated at 80 W were bumpy and remained substantially grey, suggesting that the original rough morphology of the plasma sprayed surface was not completely destroyed by the laser treatment. Since 80 W is very close to the lower limit of the operational range of the instrument, the laser treatment was performed twice on two different specimens of FGM C to verify its repeatability, which was fully confirmed, as proved by the visual analysis in Fig. 4 and also by SEM and XRD (not shown).

Even if the coatings partially maintained a bumpy morphology, the ESEM observation revealed a deep modification of the microstructure as a result of the laser treatment. Fig. 5 collects some representative ESEM images. In general, the treated surfaces became markedly cracked (Fig. 5a–c), with widespread spherical pores, which preferentially concentrated at the end of the "laser tracks" (Fig. 5f). The development of pores and cracks has already been observed in laser-treated pure HA coatings.[9,10] In particular, the microstructure of the extremely porous areas at the end of the laser tracks resembled the microstructure observed by Khor et al. in laser molten HA coatings. It was inferred that such phenomena, particularly evident at high laser power levels, could be caused by the local melting of the coating, that

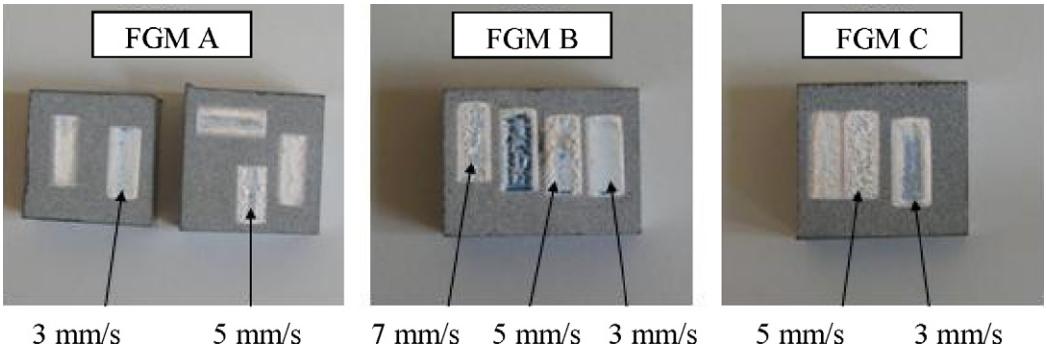

Fig. 3. Laser treatments performed at 100 W on the three preliminary graded coatings; the effect of different scanning speeds is emphasized. All the treatments were performed "in focus" and with 1 pass.

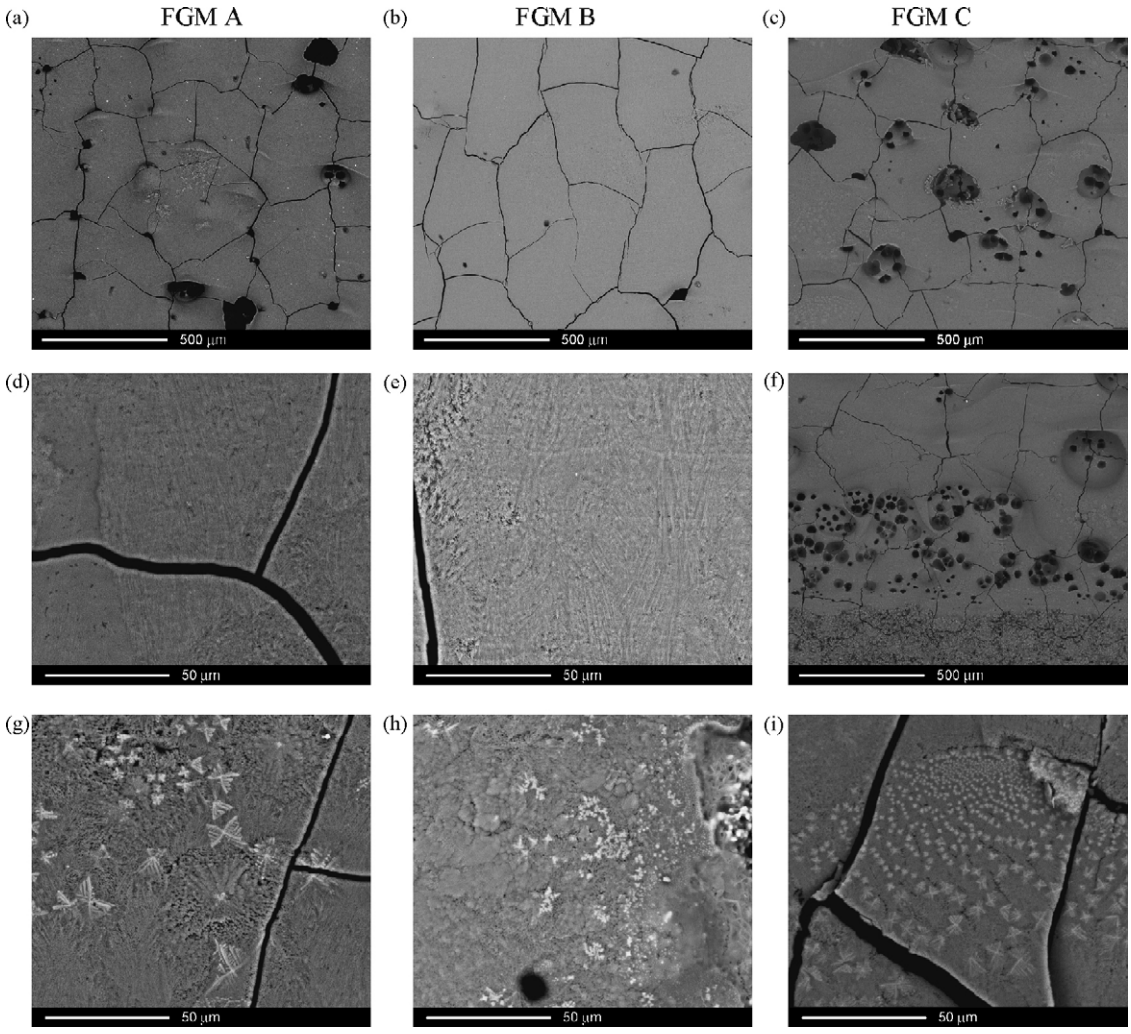

Fig. 5. ESEM images of the surfaces treated at 80 W, in focus position, 3 mm/s scan speed, 1 pass.

allows the release of entrapped gases, and the subsequent re-solidification of the molten phase, whose contraction is hindered by the underlying material.[9,10] The development of pores could be considered an interesting property of the laser treated coating as it might promote the tissue in-growth, but the abundant presence of pores, accompanied by the diffused propagation of cracks, is likely to limit the mechanical reliability of the coating.[10]

The ESEM observation also revealed several different crystal structures, with a prevalent development of white star-shaped crystals (exemplified in Fig. 5g–i), dispersed in compact grey structures (Fig. 5d and e). The XRD was required to identify the mineralogical phases developed as a consequence of the laser treatment. As shown in Fig. 6, it was possible to detect the presence of tri-calcium phosphate (TCP), perovskite ($CaTiO_3$), titanium oxide in the two polymorphs of anatase and rutile (the latter particularly abundant in FGM B but scarcely present in FGM A), and HA. It is important to underline that the laser treatment, instead of increasing the degree of crystallinity of HA, caused a decomposition of HA, inducing the development of TCP and other calcium phosphates, which reacted with the titania of the graded coating, producing the perovskite. A similar mechanism has already been observed by Kurella and Dahotre, who produced hierarchical calcium phosphate structures by means of proper laser treatments.[24] The authors pre-deposited TCP powder as a water suspension on a Ti–6Al–4V substrate and laser-processed it to obtain a textured coating. The final coat-

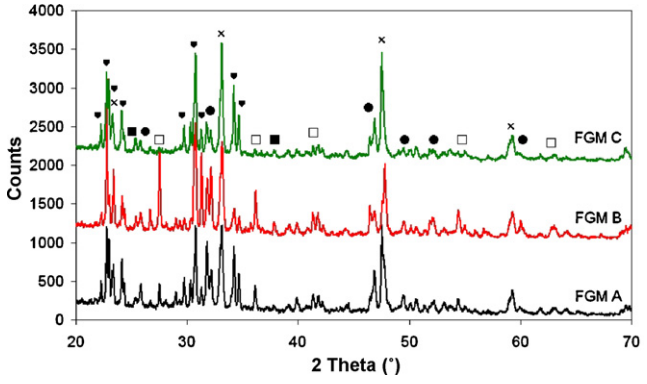

Fig. 6. XRD spectra of the preliminary coatings treated at 80 W, in focus position, 3 mm/s scan speed and 1 pass. Symbols: ▼, TCP; ×, perovskite; ■, anatase; □, rutile; ●, HA.

ing contained not only TCP, but also CaO, TiO_2 and $CaTiO_3$. Hence, it was suggested that the laser treatment, performed in ambient atmosphere, promoted the evolution of several oxides, including TiO_2 (Ti from the substrate), that reacted with Ca-rich phases producing $CaTiO_3$. Similar considerations were drawn by Paital and Dahotre, who used laser treatments for textured Ca–P coatings on titanium alloys.[25] The presence of calcium titanates is frequently detected also during laser cladding of HA on titanium alloy substrates.[24] In the present research, the reaction was probably facilitated by the presence of titania in the coating itself.

Independently of the applied power level, the multiple pass treatments gave results analogous to those of the single pass treatments (not shown); as a consequence, single pass treatments were preferred in subsequent research activities and experimental characterization.

The target of obtaining well crystallized HA surfaces and homogeneous "laser tracks" suggested to operate at low power levels and low scanning speeds. Since the laser equipment used in the present research was characterized by a rather poor beam stability when the power is set at values below 80 W, further tests were performed by de-focusing the surface to be treated.[9]

Moving the samples from the in-focus distance to −2 mm, the presence of crystalline HA increased significantly. Fig. 7 proposes a comparison between the XRD spectra of the sample FGM B treated under the same conditions (100 W, 3 mm/s, 1 pass) in focus and out of focus at −2 mm. It is apparent how the defocalization to −2 mm promoted the HA phase, whose peaks became higher, while the peaks from titania, both rutile and anatase, became almost negligible. Instead, the development of TCP and perovskite was not prevented. Such differences between the XRD graphs suggest that the reduction in the laser irradiance (power per unit of surface) achieved by defocusing could limit the decomposition of the HA. Since the HA decomposition was not completely suppressed, the resulting calcium phosphates reacted with the titania of the graded coating, producing the observed perovskite. However the "soft" laser treatment involved only the outermost surface layers of the graded coating, where the fraction of titania is relatively scarce (Fig. 1).

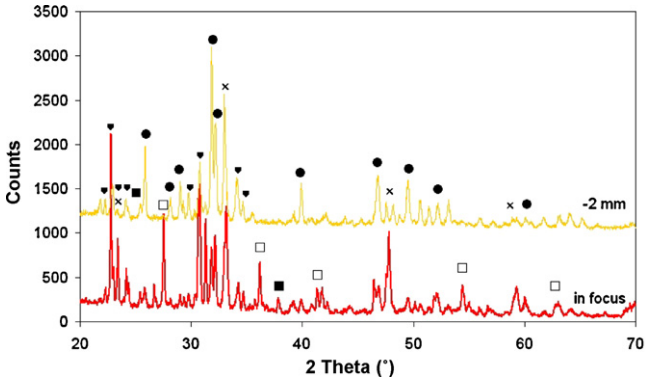

Fig. 7. Comparison between the XRD spectra of the FGM B treated at 100 W, 3 mm/s, 1 pass at different distances from the laser source: in-focus and at −2 mm. The symbols are the same as Fig. 6: ▼, TCP; ×, perovskite; ■, anatase; □, rutile; ●, HA.

As a result, all the titania was converted in the reaction with the calcium phosphate and, therefore, the rutile and anatase peaks were not present any more; instead, the calcium phosphates, specifically the TCP, partially survived the reaction with the titania, producing the aforementioned peaks in the XRD pattern.

Further defocusing of the laser beam down to −4 mm resulted in a complete suppression of the perovskite reaction. The "laser tracks" were almost invisible at the naked eye and even the ESEM investigation confirmed that the laser-treated coatings preserved their typical lamellar microstructure; an example, regarding FGM A, is presented in Fig. 8. In this way, the coating was not (re-)melted any more. Cheang et al., investigating the effect of laser treatments on pure HA coatings, described a similar mechanism, since they also observed that a reduction of the laser power changed the laser action from melting to re-crystallization.[9]

The preserved microstructure and the absence of perovskite made these treatments, performed defocusing the laser beam down to −4 mm, particularly favourable for the graded coatings. In fact, the presence of TCP does not compromise the bioactivity of the coating, but the development of perovskite

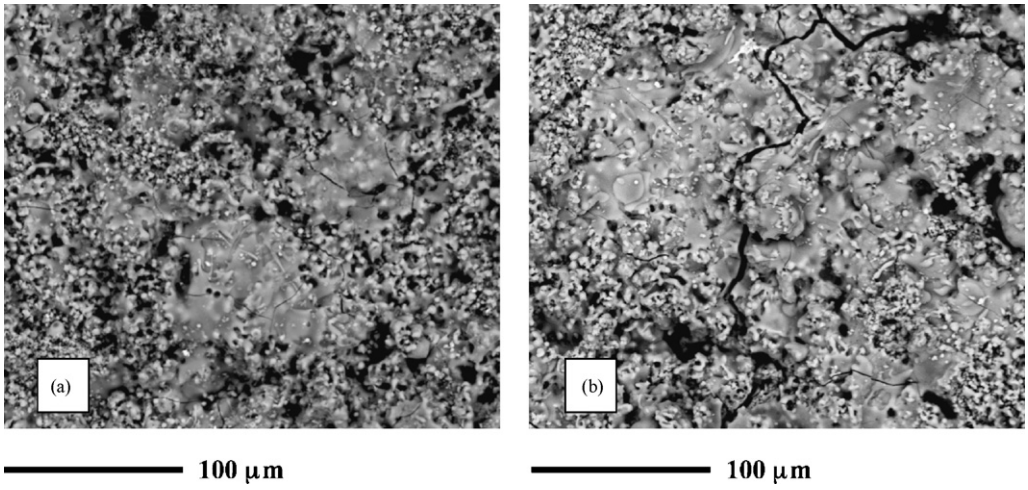

Fig. 8. Surface of FGM A before (a) and after (b) laser treatment at 100 W, −4 mm of focus distance, 3 mm/s scan speed and 1 pass.

Table 3
Selected post-deposition laser treatments performed on the final samples.

Parameters of the laser treatment				Treated samples	
Defocus (mm)	Power (W)	Speed (mm/s)	Passes (number)	FGM*	HA*
−4	100	3	1	Yes	Yes
−4	80	3	1	Yes	Yes

Columns on the left: parameters used (defocalization distance; power; traverse speed; number of passes); columns on the right: samples subjected to the specific laser treatment.

may be detrimental to deal with. The matter is still under debate, since Webster et al. observed an increased osteoblast adhesion on titanium-coated HA that developed $CaTiO_3$, but Lu et al. reported that the formation of $CaTiO_3$ is suggested to reduce adhesive strength and destroy the HA structure.[6] However, in the present research the formation of perovskite, as well as that of TCP, is not strictly controlled and hence it should be avoided. As a consequence, the most interesting sample, FGM*, and the corresponding pure HA* coating were treated by defocusing the laser beam at −4 mm according to the parameters reported in Table 3.

3.2. Final selected treatments

The microstructure (surface and cross section) of FGM* and HA*, as-sprayed and laser-treated, are presented in Figs. 9 and 10, respectively. The laser treatment did not alter the compositional gradient in FGM* and, due to the defocused laser beam, which reduced the specific power irradiating the surface, no significant cracking phenomena took place. Even after the laser treatment, FGM* retained some microstructural defects, such as pores and local points with reduced adhesion at the interface with the substrate; nevertheless, the microstructure

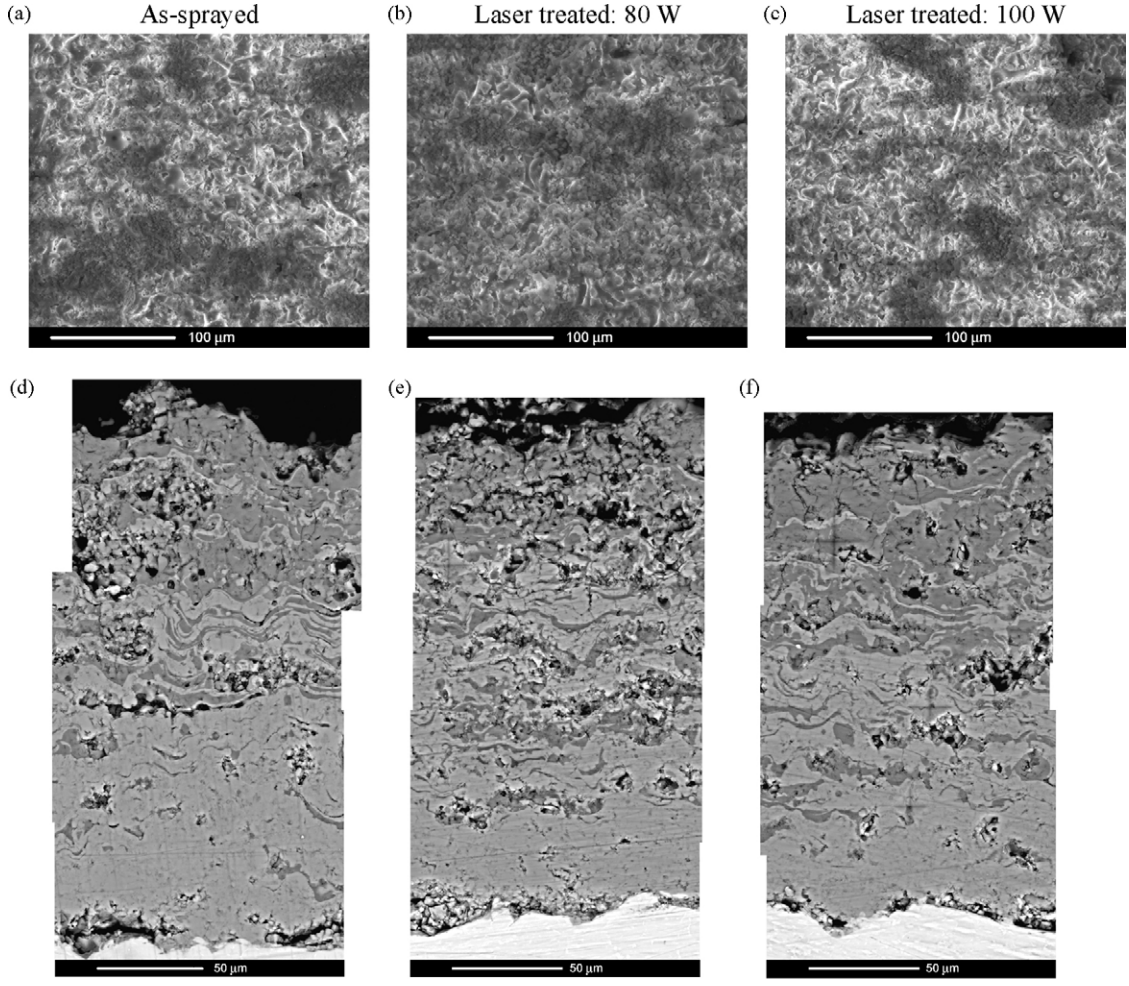

Fig. 9. Surface and cross section of FGM* as sprayed (a and d), laser treated at 80 W, −4 mm, 3 mm/s, 1 pass (b and e) and laser treated at 100 W, −4 mm, 3 mm/s, 1 pass (c and f). The images regarding the surfaces (a–c) were acquired in low vacuum mode (pressure: 0.5 Torr); those regarding the cross sections (d–f) were taken in high vacuum mode.

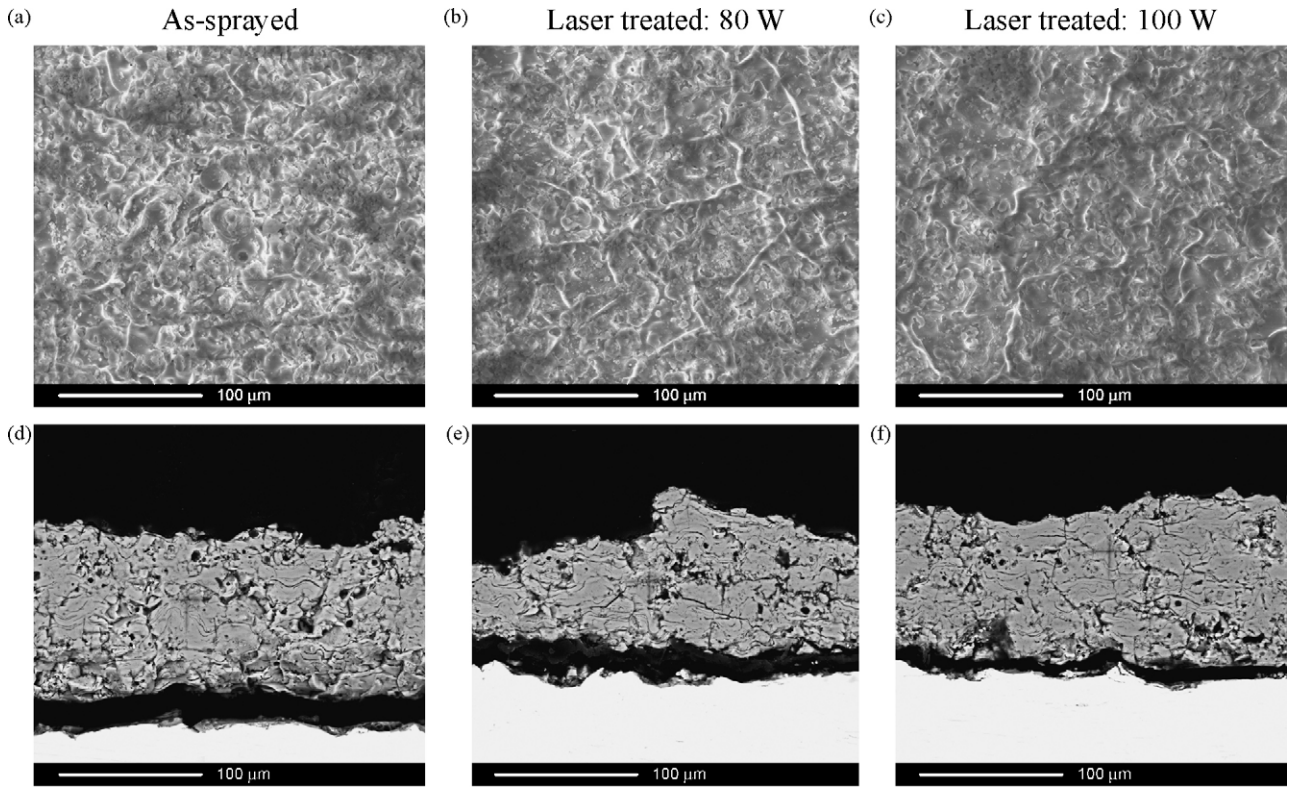

Fig. 10. Surface and cross section of HA* as sprayed (a and d), laser treated at 80 W, −4 mm, 3 mm/s, 1 pass (b and e) and laser treated at 100 W, −4 mm, 3 mm/s, 1 pass (c and f). The images regarding the surfaces (a–c) were acquired in low vacuum mode (pressure: 0.5 Torr); those regarding the cross sections (d–f) were taken in high vacuum mode.

of the titania-HA graded coating was definitely more compact than that of the HA* coating, which – before and after laser treatment – showed numerous defects and also marked through-thickness cracks. Moreover, though the deposition conditions were the same for the two coatings, the FGM* coating adhered more strongly to the substrate than the HA* one, and was also thicker and more uniform. The difference in microstructure and thickness derived from the presence of titania in the compositional gradient of FGM* and the optimisation of the spraying parameters for the graded coating.[20]

The benefits deriving from the laser treatment can be appreciated from the XRD results reported in Fig. 11 for FGM* and Fig. 12 for HA*. As regards the graded coating, the intensity of the peaks pertaining to HA was higher for the laser treated samples than for the as-sprayed one and the intensity increased with increasing power. Interestingly, no decomposition products were detected in the treated FGM*, independently of the applied power (in defocused mode, at −4 mm, the results at 80 and 100 W were similar from this point of view). On the contrary, it is worth noting that the signals caused by the TCP in the as-sprayed coating, indicated by the arrow in Fig. 11, completely disappeared after the laser irradiation. This suggests that the laser treatment performed in defocused mode at −4 mm effectively promoted the re-crystallization of the by-products derived from the thermal decomposition of HA induced by the plasma-spray processing. As shown in Fig. 12, also for the HA* coating the intensity of the HA peaks slightly increased after the laser treatment, while the peaks caused by the TCP disappeared. However, the increment was not as significant as that observed for the graded coating; most of all, the "hump" visible in the angular range 25–35° (not visible in the spectra of FGM*), which reveals the presence of amorphous phase, was not eliminated by the laser treatment. For comparison purpose, Fig. 13 directly superimposes the spectra of the samples FGM* and HA* laser treated at 100 W; the graphs highlight the presence of residual amorphous phase in the HA* coating and the higher crystallinity reached by the FGM* coating.

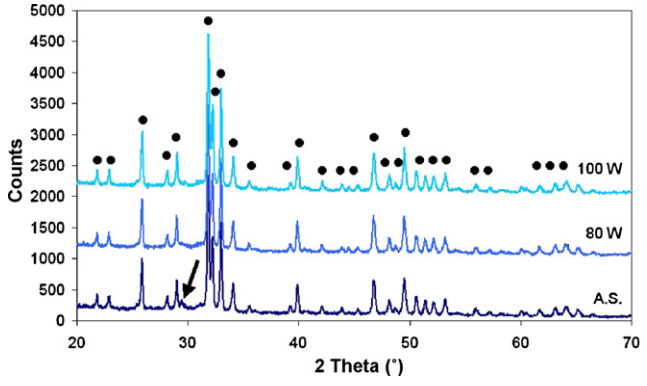

Fig. 11. XRD spectra of the sample FGM* as-sprayed and laser treated at 80 and 100 W in defocalization mode at −4 mm. The arrow indicates the signal from TCP; ● is the symbol for HA.

The indentations performed on different areas of the FGM* cross section confirmed that the compositional gradient resulted in a functional gradient, since the local Vickers hardness varied

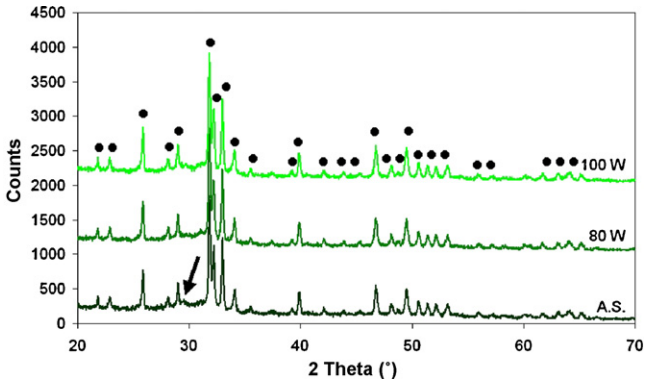

Fig. 12. XRD spectra of the sample HA* as-sprayed and laser treated at 80 and 100 W in defocalization mode at −4 mm. The arrow indicates the signal from TCP; ● is the symbol for HA.

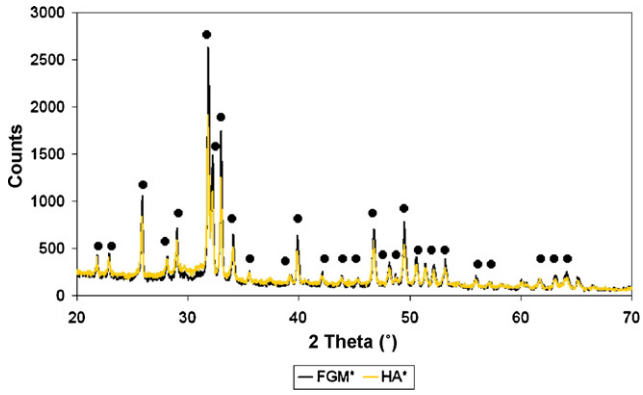

Fig. 13. Comparison between the XRD spectra of the samples FGM* and HA* laser treated at 100 W, −4 mm, 3 mm/s, 1 pass. ● is the symbol for HA.

as a function of distance from the working surface. As exemplified in Fig. 14, which refers to the indentations on the as-sprayed FGM* sample, the impressions produced by an applied load of 100 g_f were larger on the HA-rich area of the cross section, close to the working surface, than on the titania-rich area, close to the interface. Fig. 15a shows that the functional gradient was preserved by the laser treatment performed in defocalization mode, since the local hardness was not modified, independently of the laser power (80 or 100 W). It is worth noting that, independently of the laser treatment, the Vickers hardness of the HA* coating was lower than that of the HA-rich area of the FGM* cross section, as reported in Fig. 15b. In fact, the local hardness of the HA* coating ranged from about 202 HV in the as-sprayed sample to about 220 HV in the 100 W laser treated sample; instead the hardness of the HA-rich area of FGM* was about 370 HV in both the as-sprayed and laser treated samples (the difference between the three samples, as sprayed and laser treated, is negligible with respect to the experimental error).

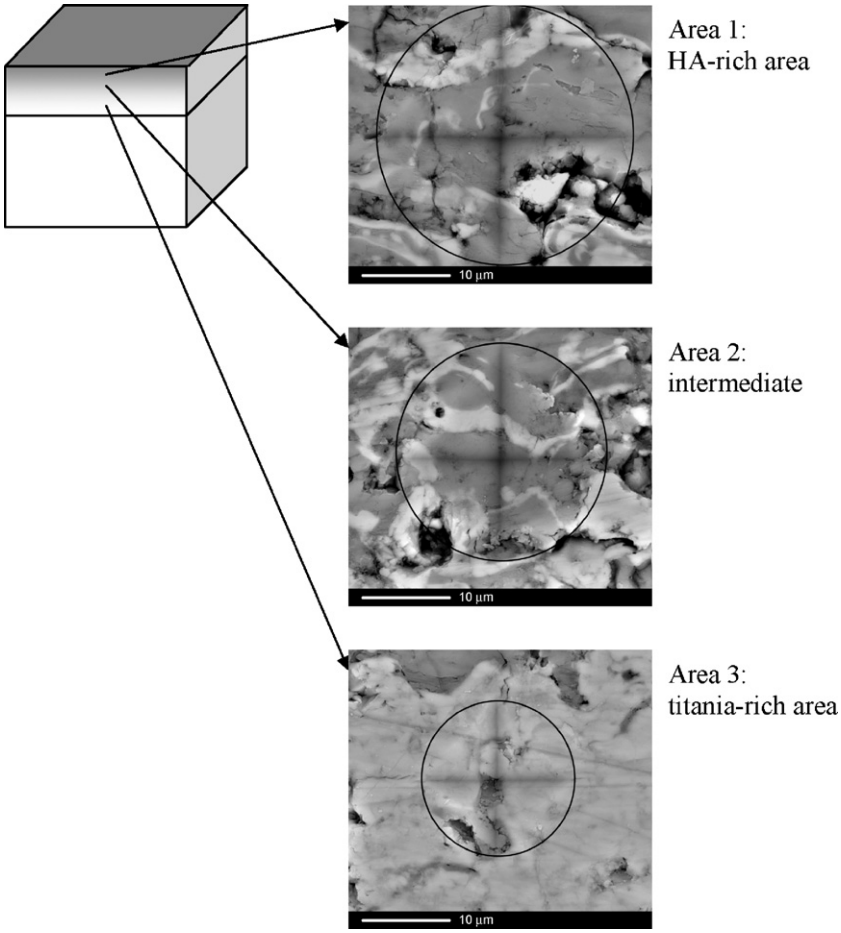

Fig. 14. Indentations performed at 100 g_f on three different areas of FGM* cross section (as-sprayed sample).

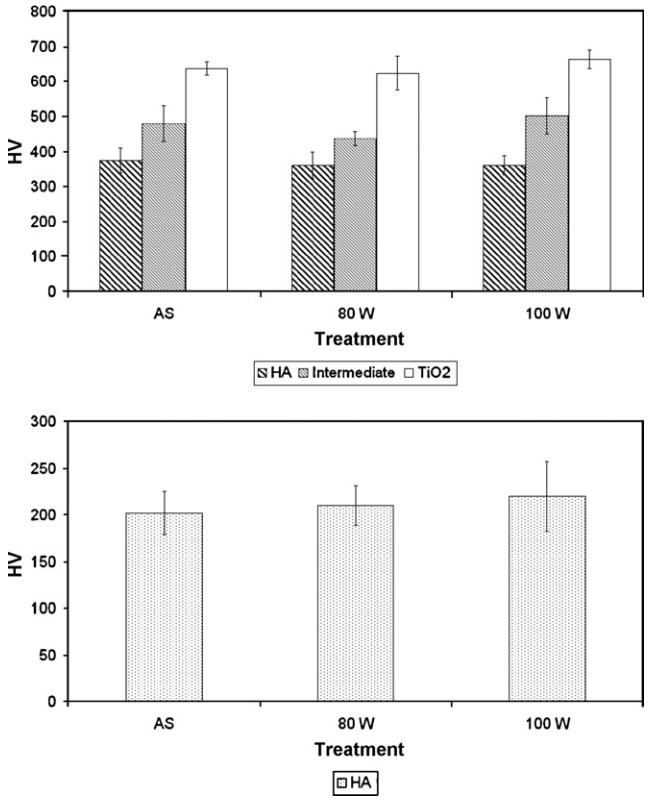

Fig. 15. Vickers microhardness (100 g_f) measured before and after laser treatment on the FGM* cross section (a), working on three different areas: HA rich; intermediate; titania rich, and on the HA* coating cross section (b).

The laser treatment, necessarily performed in defocalization mode to avoid the development of perovskite in the FGM* sample, promoted a re-crystallization of the HA, but it did not alter the microstructure or sensibly changed the local mechanical properties. In previous studies, a similar titania-HA graded coating underwent specific thermal treatments, which resulted to be beneficial not only for the degree of crystallinity, which was remarkably increased, but also for the mechanical properties of the FGM.[14,15,26] Such an improvement was not achieved by means of the laser treatment, however it was possible to increment the crystallinity of HA at the working surface in a very easy and quick way. In fact, it should be underlined that the thermal treatment is dramatically time-consuming with respect to the laser treatment.

Specific tests, in particular *in vitro* experiments by immersion in Simulated Body Fluid, are currently running; the results will be discussed in a future contribution. It is extremely important to investigate the bioactivity after the laser treatment, since a change in the degree of crystallinity could modify the surface interaction with a biological environment, as already observed for heat treated samples.[26]

4. Conclusions

Several laser treatments were performed with the purpose of incrementing the degree of crystallinity of the HA at the working surface of plasma sprayed titania-HA functionally graded coating. The governing factors were the laser power and the focus distance, which determine the specific power irradiating the sample surface and, hence, the local temperature. It was proved that excess in the specific power was disadvantageous to the coating properties, since it promoted the development of calcium phosphates that, in turn, were prone to react with the titania of the graded coating, giving place to calcium titanates (perovskite). Even if calcium phosphates are bioactive and titanium phosphates are presumably non-toxic (the effect of their presence in biomaterials is controversial), the reaction is not strictly controlled and, therefore, it should be avoided. Instead, very low values of the specific power, obtained by reducing the laser power to 80 W or 100 W and operating in defocused mode at −4 mm, eliminated the perovskite formation, increased the degree of crystallinity of HA at the working surface and even reduced the content of by-products (e.g. TCP) present in the as-sprayed samples as a consequence of the plasma spraying process. Even if the increment of the degree of crystallinity is not as high as that achieved by means of a thermal treatment, the laser treatment greatly benefits from the very short times required, seconds instead of hours and by the selectivity of treatment. In fact, the fine tuning of the laser parameters makes it possible to control the degree of crystallinity in a very strict way and, most of all, the punctual effect of the laser involves only the coating, and not the substrate, or even special selected areas of the coating surface.

Acknowledgements

The “Laser staff” at University “Tor Vergata” is gratefully acknowledged for the support to perform the laser treatments. Many thanks to Ms. Neda Kollcaku for her precious contribution to characterize the samples.

References

1. Cizek, J., Khor, K. A. and Prochazka, Z., Influence of spraying conditions on thermal and velocity properties of plasma sprayed hydroxyapatite. *Materials Science and Engineering C*, 2007, **27**, 340–344.
2. Heimann, R. B., Thermal spraying of biomaterials. *Surface & Coatings Technology*, 2006, **201**, 2012–2019.
3. Chean, P. and Khor, K. A., Addressing processing problems associated with plasma spraying hydroxyapatite coatings. *Biomaterials*, 1996, **17**, 537–544.
4. Herman, H., Sampath, S. and McCune, R., Thermal spray: current status and future trends. *MRS Bulletin*, 2000, 17–25.
5. Kurzweg, H., Heimann, R. B., Troczynski, T. and Wayman, M. L., Development of plasma-sprayed bioceramic coatings with bond coats based on titania and zirconia. *Biomaterials*, 1998, **19**, 1507–1511.
6. Lu, Yu-Peng, Li, Mu-Sen, Li, Shi-Tong, Wang, Zhi-Gang and Zhu, Rui-Fu, Plasma-sprayed hydroxyapatite + titania composite bond coat for hydroxyapatite coating on titanium substrate. *Biomaterials*, 2004, **25**, 4393–4403.
7. Wang, B. C., Chang, E., Lee, T. M. and Yang, C. Y., Changes in phase and crystallinity of plasma-sprayed hydroxyapatite coatings under heat treatment: a quantitative study. *Journal of Biomedical Materials Research*, 1995, **29**, 1483–1492.
8. Kurella, A. and Dahotre, N. B., Review paper: surface modification for bioimplants: the role of laser surface engineering. *Journal of Biomaterials Applications*, 2005, **20**(1), 5–50.
9. Cheang, P., Khor, K. A., Teoh, L. L. and Tam, S. C., Pulsed laser treatment of plasma-sprayed hydroxyapatite coatings. *Biomaterials*, 1996, **17**, 1901–1904.

10. Khor, K. A., Vreeling, A., Dong, Z. L. and Cheang, P., Laser treatment of plasma sprayed HA coatings. *Materials Science and Engineering*, 1999, **A266**, 1–7.
11. Chen, C., Wang, D., Bao, Q., Zhang, L. and Lei, T., Influence of laser remelting on the microstructure and phases constitution of plasma sprayed hydroxyapatite coatings. *Applied Surface Science*, 2005, **250**, 98–103.
12. Dyshlovenko, S., Pierlot, C., Pawlowski, L., Tomaszek, R. and Chagnon, P., Experimental design of plasma spraying and laser treatment of hydroxyapatite coatings. *Surface and Coating Technology*, 2006, **201**, 2054–2060.
13. Feddes, B., Vredenberg, A. M., Wehner, M., Wolke, J. C. G. and Jansen, J. A., Laser-induced crystallization of calcium phosphate coatings on polyethylene (PE). *Biomaterials*, 2005, **26**, 1645–1651.
14. Perriere, J., Millon, E. and Fogarassy, E., *Recent Advances in Laser Processing of Materials (European Materials Research Society Series)*. Elsevier Ltd., Kidlington, Oxford, UK, 2006.
15. Fenineche, N. E. and Cherigui, M., In *Thermal Spraying Coatings Assisted by Laser Treatment LASER AND PLASMA APPLICATIONS IN MATERIALS SCIENCE: First International Conference on Laser Plasma Applications in Materials Science-LAPAMS'08. AIP Conference Proceedings, vol. 1047*, 2008, pp. 95–98.
16. Antou, G., Montavon, G., Hlawka, F., Cornet, A., Coddet, Ch. and Machi, F., Modification of ceramic thermal spray deposit microstructures implementing in situ laser remelting. *Surface and Coatings Technology*, 2003, **172**, 279–290.
17. Park, J. H., Kim, J. S., Lee, K. H., Song, Y. S. and Chang Kang, M., Effects of the laser treatment and thermal oxidation behavior of CoNiCrAlY/ZrO2–8 wt%Y_2O_3 thermal barrier coating. *Journal of Materials Processing Technology*, 2008, **201**(1–3), 331–335.
18. Lin, Li, The advances and characteristics of high-power diode laser materials processing. *Optics and Lasers in Engineering*, 2000, **34**(4–6), 231–253.
19. Cannillo, V., Lusvarghi, L. and Sola, A., Production and characterization of plasma sprayed TiO_2-hydroxyapatite functionally graded coatings. *Journal of the European Ceramic Society*, 2008, **28**, 2161–2169.
20. Cannillo, V., Lusvarghi, L. and Sola, A., Design of experiments (DOE) for the optimisation of titania-hydroxyapatite functionally graded coatings. *International Journal of Applied Ceramic Technology*; in press, doi:10.1111/j.1744-7402.2008.02298.x.
21. Montgomery, D. C., *Design and Analysis of Experiments*. Wiley, New York, 2001.
22. Mohammadi, Z., Ziaei-Moayyed, A. A. and Sheikh-Mehdi Mesgar, A., Adhesive and cohesive properties by indentation method of plasma-sprayed hydroxyapatite coatings. *Applied Surface Science*, 2007, **253**, 4960–4965.
23. Miyamoto, Y., Kaysser, W. A., Rabin, B. H., Kawasaki, A. and Ford, R. G., *Functionally Graded Materials. Design, Processing and Applications*. Kluwer Academic Publishers, 1999.
24. Kurella, A. and Dahotre, N. B., Laser induced hierarchical calcium phosphate structures. *Acta Biomaterialia*, 2006, **2**, 677–683.
25. Paital, S. R. and Dahotre, N. B., Laser surface treatment for porous and textured CaP bio-ceramic coating on Ti–6Al–4V. *Biomedical Materials*, 2007, **2**, 274–281.
26. Cannillo, V., Lusvarghi, L., Pierli, F. and Sola, A., In-vitro behaviour of titania-hydroxyapatite functionally graded coatings. *Advances in Applied Ceramics*, 2008, **107**(5), 259–267.